# Waveform-Space-Time Adaptive Processing for Distributed Aperture Radars

Raviraj S. Adve, Dept. of Elec. and Comp. Eng., University of Toronto
Richard A. Schneible, Stiefvater Consultants, Marcy, NY
Gerard Genello, Sensors Directorate, Signal Processing Branch, US Air Force Research Laboratory
Paul Antonik, Sensors Directorate, Signal Processing Branch, US Air Force Research Laboratory,

Key Words: Distributed apertures, Waveform Diversity

*ABSTRACT*

This paper presents the preliminary development of adaptive signal processing for distributed, waveform diverse, antenna arrays. The long term goal is to develop practical waveform-time-space adaptive processing algorithms for distributed apertures. A crucial issue identified in previous works is that, in practice, the target and interfering sources are not in the far-field of the antenna array. Recent work by the authors develops the model required to generate simulated data. This paper extends this work, focusing on using the model to formulate adaptive signal processing algorithms specifically for waveform diverse distributed apertures.

## I. Introduction

In the field of radar signal processing, a recent exciting proposal has been to combine the benefits of extremely sparse arrays with the benefits of waveform diversity. Such a system is based on an array of sub-apertures placed several thousands of wavelengths apart. Waveform diversity has been proposed to deal with the resulting problems of grating lobes. Each sub-aperture of the array transmits a unique waveform, orthogonal to waveforms transmitted by the other apertures. Initial studies have shown that while providing a remarkably narrow main-beam, such a system can also eliminate grating lobes [1, 2].

So far, research into waveform diverse distributed apertures has mainly been for proof-of-concept. In the area of adaptive signal processing for such systems, in particular, the studies have been limited and have generally ignored the specifics of distributed apertures [1, 3]. Existing space-time-adaptive processing (STAP) algorithms were applied to the waveform-time-space adaptive processing (WTSAP) case. Waveform diversity is achieved using multiple narrow band transmissions. While the results were promising, in general, the studies serve more to highlight the work remaining in developing practical adaptive processing for waveform diverse distributed apertures.

A very important result that came out of the work in [1, 2], is that given the extremely long baselines (thousands of wavelengths), the ranges of interest are not in the far field of the antenna array, indeed the entire notion of a steering vector has to be revisited. The range dependence of target and interference has significant impact on the performance of adaptive algorithms and requires the formulation of algorithms specifically to address this issue.

In developing adaptive signal processing for airborne radar arrays, a crucial development was the availability of data models for the target and interference [4]. A recent contribution in [5] was a similar model for the case wherein the steering vector is a function of range. To account for the frequency diversity, the processing scheme uses true time delay between the widely distributed apertures. The interference is modelled as a sum of several low power interference sources, each with a range dependent contribution to the overall interference. This paper presents results of preliminary investigations into using adaptive processing using this model to generate data. The examples demonstrate the importance of frequency diversity in eliminating grating lobes.

This paper is organized as follows. Section 2 illustrates the problem and introduces the system model used for the steering vector and the interference model. Section 3 presents results of numerical simulations using the model developed in Section 2. Section 4 concludes the paper and points to future work.

## 2. *SYSTEM MODEL*

In the case of airborne radar, all sources are in the far-field and the steering vector depends only on the *angle* between the source direction and the array baseline. The data model, such as that developed in [4], for both target and interference depends heavily on the use of such a steering vector. The situation is not as simple for distributed arrays. Given an antenna array with largest dimension $D$, operating at wavelength $\lambda$, the distance to the far field must satisfy [6]

$$r \gg D, \tag{1}$$
$$r \gg \lambda, \tag{2}$$
$$r \gg 2D^2/\lambda. \tag{3}$$

Using typical values for distributed apertures, $D = 200$m, $\lambda = 0.03$m, implies that the far field begins at a distance of approximately 2700km. Clearly for widely distributed apertures, both targets and interfering sources are *not in the far field*. This fact requires that any analysis of waveform diverse apertures start "from scratch". The notion of a steering vector still exists, but now depends on both angle *and range*, i.e., *each point* in space corresponds to in its own steering vector. Furthermore, coherent processing of the signals over the distributed array

with frequency diversity requires true time delays, as opposed to the phase shifts used in narrowband processing. Formulating the steering vector requires accounting for these issues.

### 2.1 *System Model and Steering Vector*

The model of the distributed aperture assumes the array comprise $N$ elements distributed over the $x-y$ plane, at points $(x_n, y_n), n = 1, \ldots, N$. Each element in the array transmits a coherent stream of $M$ linear-FM pulses, with common bandwidth $B$ with pulse repetition interval (PRI) $T_r$. However, each element transmits at a different central frequency $f_n, n = 1, \ldots N$. The transmission scheme uses true time delay to focus on a look-point $(X_t, Y_t, Z_t)$. This is in contrast to an airborne radar wherein a transmitting array uses phase shifts to transmit in a look direction. The return signal at all $N$ frequencies is received and processed at all $N$ elements, i.e., the return signal over space, time and frequency can be written as a length-$N^2M$ vector. The model developed here was initially proposed in [5] and is summarized here for completeness.

The receiver uses true time delay to coherently process all $N$ frequencies. Denote as $D_n = \sqrt{(X-x_n)^2 + (Y-y_n)^2 + (Z-z_n)^2}$, the distance of the look point to the $n^{\text{th}}$ element. The time delay used by the $n^{\text{th}}$ element on receive is

$$\Delta T_n = \frac{\max\{D_n\} - D_n}{c}, \tag{4}$$

where $c$ is the speed of light. This is the time delay introduced to the signal at the $n^{\text{th}}$ receive element. By using true time delay, the normalized response at the $N$ elements due to all $N$ frequencies for a target at the look point is just a vector of ones, i.e., the space-time-frequency steering vector, $\mathbf{s}$, is given by

$$\mathbf{s} = \mathbf{s}_t \otimes \mathbf{s}_{sf}, \tag{5}$$

$$\mathbf{s}_t = \left[1,\, e^{j2\pi f_d T_r}, \ldots, e^{j(M-1)\times 2\pi f_d T_r}\right]^T, \tag{6}$$

$$\mathbf{s}_{sf} = [1,\, 1,\, 1, \ldots, 1]^T, \tag{7}$$

where $\otimes$ denotes the Kronecker product, $f_d$ the target Doppler frequency, $\mathbf{s}_t$ the length-$M$ temporal steering vector as in [4] and $\mathbf{s}_{sf}$ the length-$N^2$ space-frequency steering vector of ones.

### 2.2 *Interference Model*

As in the case of airborne radar [4], interference here is modelled as the sum of many low power sources. However, due to frequency diversity and true time delay, the interference model is far more complex than in the airborne radar case. We begin by deriving the contribution for an individual interference source for one frequency $f_n$. The transmitted signal over $M$ coherent pulses with pulse shape $u_p(t)$ is given by

$$s(t) = u(t)e^{j2\pi f_n t + \psi}; u(t) = \sum_{m=0}^{M-1} u_p(t - mT_r), \tag{8}$$

where $\psi$ is a random phase shift. The received signal at element $i$ due to this transmitted signal at frequency $f_n$ is

$$\tilde{r}_i^n(t) = A_c u(t - \tau_i) e^{j2\pi(f_n + f_{dc})(t-\tau_i)}, \tag{9}$$

where $A_c$ is the complex amplitude, with random phase (also incorporating $\psi$), $f_{dc}$ the Doppler frequency of the interference source and $\tau_i = \left(\sqrt{(x_i - x^l)^2 + (y_i - y^l)^2 + (z_i - z^l)^2}\right)/c$ is the delay from the $l^{\text{th}}$ interference source to the $i^{\text{th}}$ element. After down-conversion and delaying the signal by $\Delta T_i$, the baseband signal at element $i$ is

$$\begin{aligned} r_i^n(t) &= A_c u(t - \tau_i - \Delta T_i) e^{-2\pi f_n(\tau_i + \Delta T_i)} \\ &\times \quad e^{j2\pi f_{dc} t} e^{-j2\pi f_{dc}(\tau_i + \Delta T_i)}. \end{aligned} \tag{10}$$

After matched filtering with the time reversed pulse shape, the signal becomes

$$x_i^n(t) = \int_{-\infty}^{\infty} r_i(\tau) u_p^*(\tau - t) d\tau, \tag{11}$$

$$\begin{aligned} &= \sum_{m=0}^{M-1} A_c e^{-j2\pi f_n(\tau_i + \Delta T_i)} e^{jm2\pi f_{dc} m T_r} \times \\ &\qquad \int_{-\infty}^{\infty} u_p(\tau - \tau_i - \Delta T_i - mT_r) u_p^*(\tau - t) \\ &\qquad\quad e^{j2\pi f_{dc}(\tau - \tau_i - \Delta T_i - mT_r)} d\tau. \end{aligned} \tag{12}$$

The final integral is recognized as the ambiguity function of the pulse shape evaluated at the interference source Doppler $f_{dc}$. Therefore,

$$\begin{aligned} x_i^n(t) &= \sum_{m=0}^{M-1} A_c e^{-j2\pi f_n(\tau_i + \Delta T_i)} e^{j2\pi f_d m T_r} \\ &\qquad \chi(t - mT_r - \tau_i - \Delta T_i, f_{dc}), \end{aligned} \tag{13}$$

where $\chi(\tau, f)$ is the ambiguity function of the pulse shape $u_p(t)$ evaluated at delay $\tau$ and Doppler $f$. Sampling this signal every $t = kT_s$ corresponding to each range bin and using $\chi(mT_r, f) \simeq 0, m \neq 0$,

$$\begin{aligned} x_i^n(kT_s) &= \sum_{m=0}^{M-1} A_c e^{-j2\pi f_n(\tau_i + \Delta T_i)} e^{j2\pi f_d m T_r} \\ &\qquad \chi(kT_s - mT_r - \tau_i - \Delta T_i, f_{dc}), \end{aligned} \tag{14}$$

Finally, given $N_c$ interfering sources at location $\{x^l, y^l, z^l\}_{l=1}^{N_c}$ with corresponding Doppler frequency $f_{dc}^l$, the received signal the $i^{\text{th}}$ element on the $m^{\text{th}}$ pulse at frequency $f_n$ is

$$\begin{aligned} x_i^n(kT_s, m) &= \sum_{l=1}^{N_c} A_c^l e^{-j2\pi f_n(\tau_i^l + \Delta T_i)} e^{j2\pi f_n^l m T_r} \\ &\qquad \chi(kT_s - \tau_i^l - \Delta T_i, f_{dc}^l), \end{aligned} \tag{15}$$

Note that $\Delta T_i$, defined in Eqn. (4), remains the delay from the *look point* to the $i^{\text{th}}$ element.

## 3. *NUMERICAL SIMULATIONS*

The development of the model in Section 2 is motivated by a desire to develop adaptive processing for the case of waveform diverse, distributed apertures This section presents the results

TABLE I

PARAMETERS COMMON TO ALL EXAMPLES

| Parameter | Value | Parameter | Value |
|---|---|---|---|
| $N$ | 16 | $M$ | 8 |
| $B$ | 10MHz | $T_p$ | $10\mu s$ |
| PRI | $5T_p$ | Target SNR | 10dB |
| Target Velocity | 50m/s | Freq. Offset | 100MHz |
| $X_t$ | -86.51m | $Y_t$ | -333.12m |
| $Z_t$ | 200km | INR | 50dB |

of numerical simulations using the model developed above. In keeping with the nascent nature of this research area, the examples are preliminary in nature focusing on the fully adaptive processing scheme [4]. The examples serve to illustrate the importance of frequency diversity and the need for range dependent adaptive processing. However, the first example illustrates the importance of frequency diversity using the non-adaptive, matched filter. The data does not include interference.

All examples use the same parameters, shown in Table I. The array uses a nominal center frequency of 10GHz. In the table $T_p$ refers to the duration of each linear-FM up-chirp. The frequency offset is the difference between carrier frequencies of the $N$ transmissions. The array elements are uniformly distributed in the $x-y$ plane on a square $200m \times 200m$ grid. The interference-to-noise ratio (INR) is relevant only if interference data is included in the simulation.

### 3.1 *Example 1: Need for Frequency Diversity*

This example illustrates the need for frequency diversity, without considering interference. The data includes a sum of a target and additive white Gaussian noise (AWGN). The target is at a range of 200km, in the radial ($z$) direction. Figure 1 plots the beampattern in the transverse, $x-$direction at the target range. It should be mentioned that since the steering vectors are range dependent, the beampattern is in fact a plot of the signal strength versus the transverse coordinate. Note the closely spaced grating lobes. The range dependence of the steering vector results in a very small decay in the grating lobe level further away from the target location $X_t$. However, clearly, the decay is inadequate for purposes of target detection. Figure 2 plots the beampattern in the radial $z$-direction. As expected, grating lobes do not occur.

Figures 3 and 4 plot the beampatterns when including frequency diversity. As seen in Fig. 3, the use of frequency diversity eliminates the grating lobes. Note, also, the asymmetrical beampattern due to the range dependence. Figure 4 illustrates the significant improvement in range resolution on using frequency diversity, coupled with true time delay processing.

### 3.2 *Example 2: Need for Adaptive Processing*

This example illustrates the effect of interference and the use of adaptive processing. The array uses 16 elements equally spaced in $x$ and $y$ coordinates. The overall length of the array in each dimension is $200m$. Interference is modelled as a spherical cluster of $10^4$ low power interfering sources offset from the target location in the transverse direction by 1.6km. The radius of the interference cluster is set to 400m.

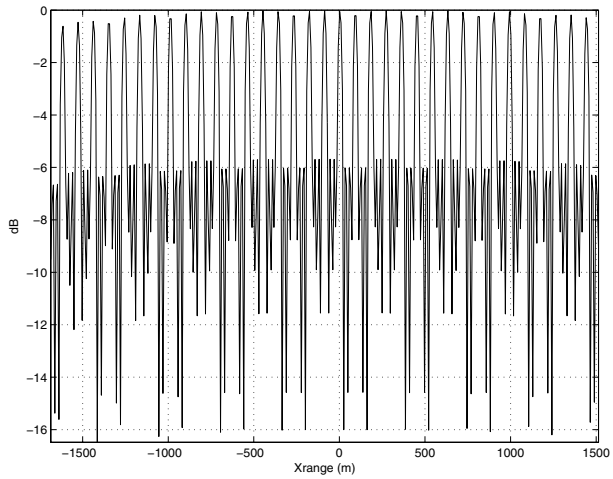


Fig. 1. Matched filter processing along the transverse, $x$-direction. No frequency offset.

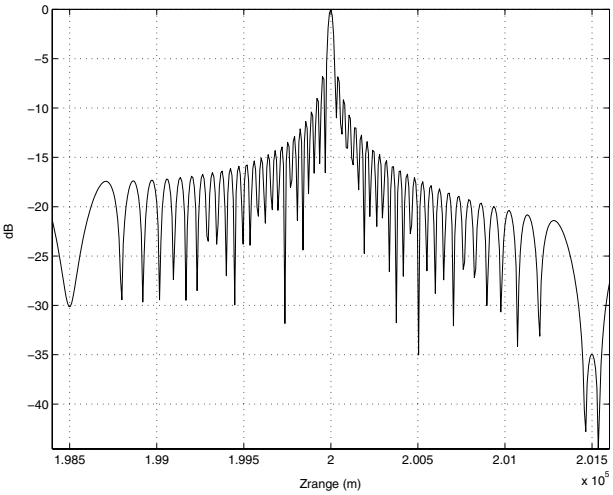


Fig. 2. Matched filter processing along the radial, $z$-direction. No frequency offset.

Figure 5 plots the results of non-adaptive processing as a function of the transverse, $x-$direction, Figure 6 plots similar results for the radial $z$-direction. As is clear, the strong interference completely buries the weak target. The non-adaptive pattern in the radial direction clearly indicates the extent of the interference sources.

Figure 7 plots the modified sample matrix inversion (MSMI) statistic [4] as a function of the transverse $x$-direction. The limited interference range limits the available secondary data. This adaptive processing therefore uses only $M = 3$ pulses in the CPI. All interference range cells are used to estimate the interference covariance matrix. Note that even with using three pulses, the target is clearly identified within interference. Figure 8 plots the MSMI statistic versus the radial, $z$-dimension. As compared to Fig. 6, the target is clearly detected with signif-

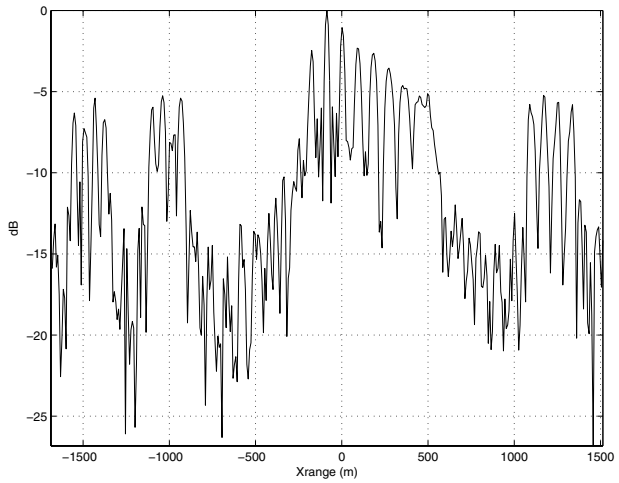


Fig. 3. Matched filter processing along the transverse, $x$-direction.

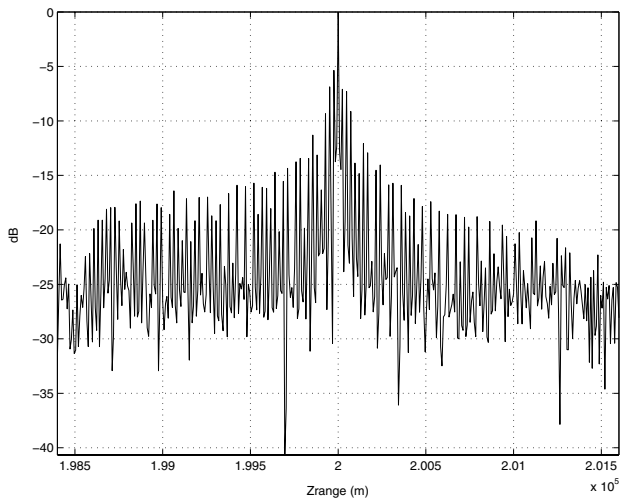


Fig. 4. Matched filter processing along the radial, $z$-direction.

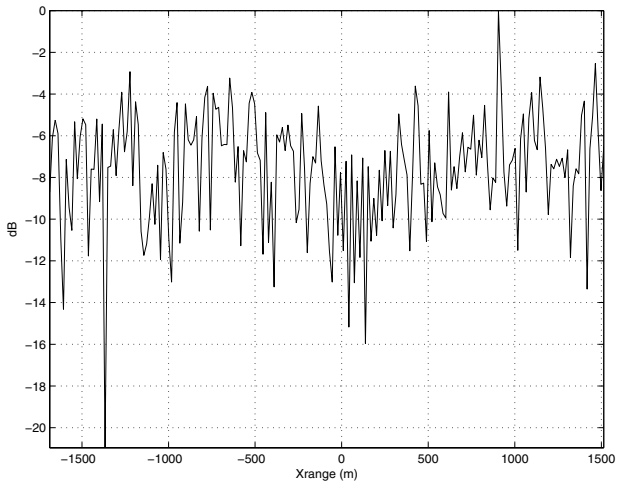


Fig. 5. Matched filter processing along the transverse, $x$-direction. Includes interference.

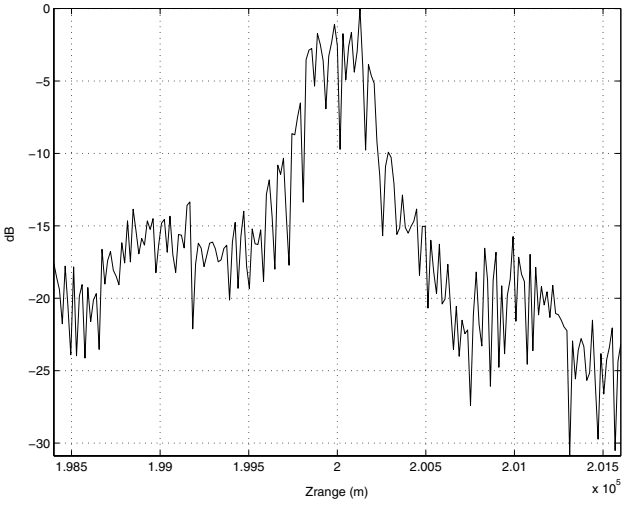


Fig. 6. Matched filter processing along the radial, $z$-direction. Includes interference.

icantly improved range resolution.

## II. Conclusions and Future Work

This paper has taken the initial steps toward developing adaptive processing for distributed aperture, frequency diverse, arrays. The steps are parallel to those undertaken in the 1990s that proved successful in the development of STAP for airborne radar, starting with the development of a data model [4]. Based on the realization that the target and interfering source are not in the far-field of the array, this paper develops a data model accounting for range dependence while accounting for true time delay for multiple frequency bands. The numerical examples illustrate the importance of having such a data model. The data model is used here to estimate the beampattern and beamwidths in both the transverse and radial directions. The model is also used in a single numerical example illustrating the importance of adaptive processing for distributed aperture arrays.

The numerical results illustrate the crucial differences from STAP for airborne radar and the work remaining to develop a good understanding of adaptive processing for distributed apertures. As the second example shows, in crucial interference scenarios of interest, the availability of secondary data is a crucial issue. It is, therefore, likely that available adaptive algorithms, developed for airborne radar, are not relevant to the application at hand. The long-term goal of this effort is the development of adaptive algorithms *specifically* for distributed aperture, frequency diverse, arrays.

## References

[1] R. S. Adve, "Adaptive processing for distributed aperture radars," in *Proc. of the 1st Waveform Diversity Workshop*, Feb. 2003. NRL, Washington, DC.

[2] R. S. Adve, R. A. Schneible, and R. McMillan, "Adaptive space/frequency processing for distributed apertures," in *Proc. of 2003 IEEE Radar Conference*, May 2003. Huntsville, AL.

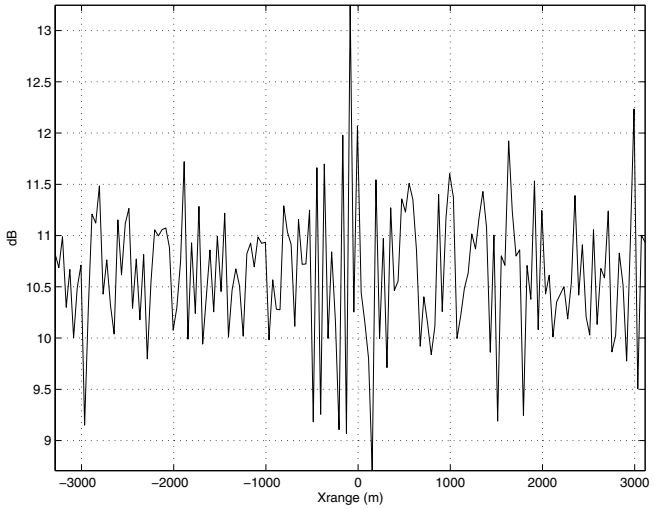


Fig. 7. MSMI statistic versus transverse $x$-dimension. Includes interference.

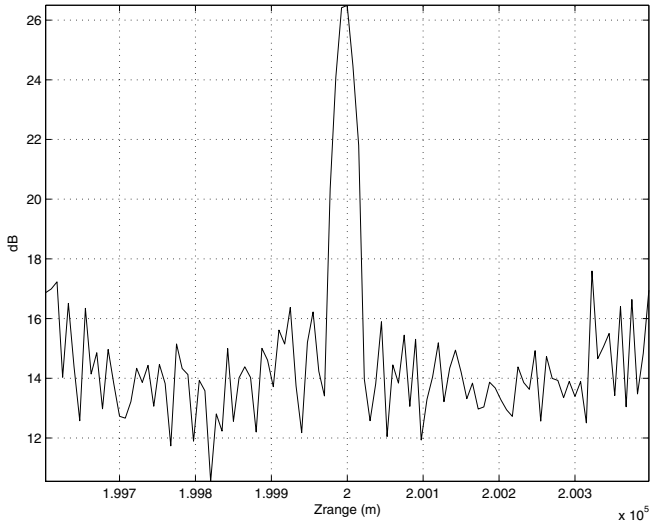


Fig. 8. MSMI statistic versus radial $z$-dimension. Includes interference.

[3] R. S. Adve, "Sub-optimal adaptive processing for distributed aperture radars," in *Proc. of the 2nd Waveform Diversity Workshop*, Feb. 2004. Verona, NY.

[4] J. Ward, "Space-time adaptive processing for airborne radar," Tech. Rep. F19628-95-C-0002, MIT Linclon Laboratory, December 1994.

[5] R. S. Adve, R. Schneible, M. C. Wicks, and R. McMillan, "Adaptive processing for distributed aperture radars," in *Proc. of 1st Annual IEE Waveform Diversity Conference*, Nov. 2004. Edinburgh.

[6] C. Balanis, *Antenna Theory: Analysis and Design*. John Wiley, 1997.